

Archaeo-geophysical survey and magnetic modelling of a mound on the southern rim of Castiglione crater (Italy)

F. FLORINDO¹, V. SAPIA², R. DE RITIS², A. WINKLER², S. HELAS³ and M. DI NEZZA²

¹ Gruppo Archeologico Latino "Latium Vetus", Monte Porzio Catone, Roma, Italy

² Istituto Nazionale di Geofisica e Vulcanologia, Roma, Italy

³ Institut für Archäologie und Kulturanthropologie, Universität Bonn, Germany

(Received: 13 July 2017; accepted: 29 June 2018)

ABSTRACT We present the preliminary results of a geophysical investigation applied to the subsoil imaging of a morphological height (here described as *mound*) within the area of the ancient city of Gabii, situated 18 km to the east of Rome, and its near surroundings. Interpolated magnetic data revealed the presence of a dipolar magnetic anomaly in correspondence of the *mound*, which we interpret to be the response of a high intense magnetic sources, with a regular, almost rectangular, geometry, lying approximately at the base of the *mound*. In particular, forward magnetic modelling solutions suggest that this magnetic dipole could be presumably caused by a basal peperino plateau magnetized along the Earth's present-day magnetic field. In the surroundings, magnetic results showed a series of intense dipolar magnetic anomalies, N-S oriented, arranged to form a linear road-like pattern which we attribute as due to leucititic lava stones buried at very shallow depth. Obtained results are encouraging. We believe that further geophysical investigations will be crucial to better characterize the inner structure of a potentially relevant archaeological feature.

Key words: Gabii, magnetic anomaly, magnetic modelling, Castiglione crater, *mound*.

1. Introduction

Gabii was an ancient city of the Latins, the Italic people who inhabited the region defined as *Latium Vetus*, approximately corresponding to the territory of modern Latium south of the Tiber River. The settlement sits on the south-eastern edge of the Castiglione volcanic crater, an eccentric feature of the Colli Albani Complex, about 18 km to the east of Rome on the ancient Via Praenestina (the road connecting Rome to Praeneste, in origin named Via Gabina). The area is crossed by streams, most notably Fosso dell'Osa and Fosso di San Giuliano (respectively on the western and eastern sides of the crater), tributaries of the Aniene River which are thought to have once been navigable (Bietti Sestieri, 1992), and it was once characterized by the presence of two major water bodies: Lake Castiglione, which occupied the omonymous crater, and the palustrine wetland basin of Pantano (also known as *Pantano Secco* or *Pantano Borghese*), south of the Praenestina (Becker *et al.*, 2009; Angle and Mancini, 2010). Both of these water bodies have been drained by the Borghese family, respectively in the 20th and 17th centuries (Aglietti, 2002).

Within the ancient settlement area, on the southern edge of the crater rim, lies a *mound* (here used as synonym of small hillock and with no real archaeological preconception; hereinafter always in italics) whose dimensions and slope are conspicuously regular. Its present-day dimensions are approximately 10 m in height and about 55-60 m in diameter, with the E-W section being slightly larger than the N-S one. The elevation is already clearly marked on a map by Adolfo Cozza, which was published as part of the catalogue of known archaeological remains of Gabii (Cozza and Pasqui, 1885), and later recorded on a map by Giovanni Pinza, labelled as «Tumulo» (Pinza, 1903).

The limited dimensions of the *mound* and the absence of scoria (fragments of solidified lava) on and around it lead us to exclude that its morphology is attributable to a scoria cone. Because of its location within a dense archaeological scenario, and considering that it lies in a prominent position on the side of a major ancient roadway, determining the nature of the *mound* is a matter of extreme interest for the general understanding of the past human exploitation of the area.

In April 2008 the German Archaeological Institute in Rome has promoted a preliminary geophysical survey by means of an electrical resistivity tomography over the *mound* area, which has been carried out by researchers from the University of Kiel. In general, the recovered resistivity models (not shown here) revealed the existence of regular, differentiated electrical resistivity structures within the *mound*. The core of the hill has resulted as a zone of high resistivity, followed by a transitional zone of low resistivity and a narrower strip of high resistivity responses close to the surface, covering the entire structure (Erkul E., University of Kiel, confidential report).

In order to further investigate the nature of the *mound*, we carried out a magnetic survey (Fig. 1) with the aim to: a) highlight the presence of magnetic anomalies as due to a susceptibility

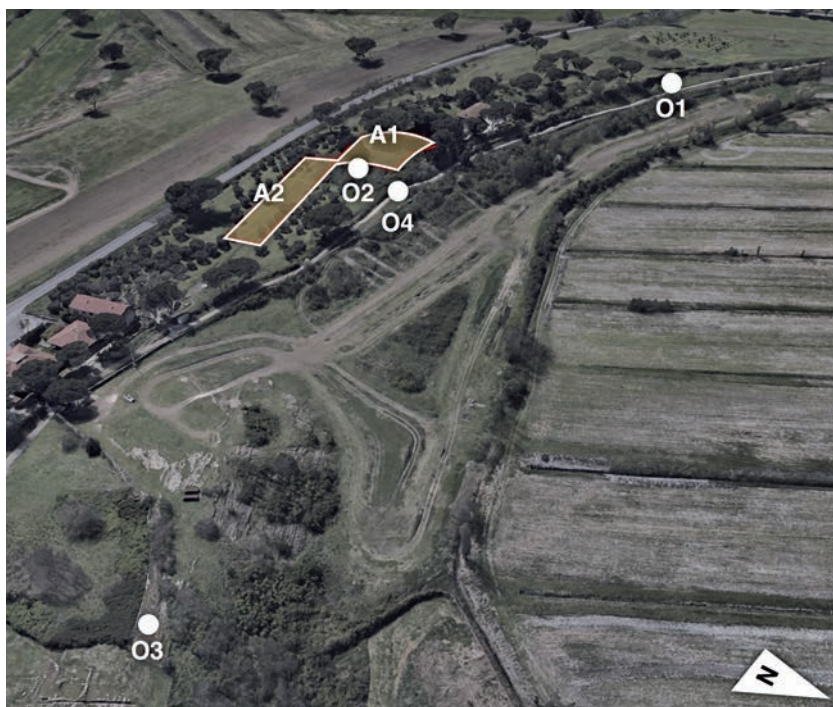


Fig. 1 - Satellite map of the magnetic survey area with the location of the four outcrops (white dots, O1-O4) which were sampled and analysed. A1 corresponds to the *mound* survey area while A2 to its near surrounding.

contrasts within the *mound* itself; b) map the surrounding area in search for further buried traces of past human activity. The same geophysical method has already been successfully applied to characterize an archaeological *mound*, notwithstanding a weak magnetic signature of the archaeological feature and the host rock was observed (Ioane *et al.*, 2009). We also propose synthetic modelling of the magnetic anomaly field which provided us important clues to interpret and speculate to possible origin of this morphological height. To constrain the forward modelling, we carried out on field susceptibility measurements of outcropping volcanic deposits, including one placed at the base of the *mound*, using a portable susceptibility meter. In addition, these outcrops have been sampled and analysed at the Istituto Nazionale di Geofisica e Vulcanologia (INGV) paleomagnetism laboratory in order to characterize the magnetic mineralogy and to establish its lateral continuity.

2. Study area

2.1. Archaeological setting

The remains of the Latin city lie within a wider archaeological context which has been defined as Gabii-Osteria dell'Osa-Castiglione district (Bietti Sestieri, 1992), hereinafter GOOCD. The earliest archaeological evidence within the GOOCD is the Middle and Late Bronze Age settlement located on the internal eastern slope of the Castiglione crater (Bietti Sestieri, 1992). Early Iron Age evidence is more quantitatively relevant and extremely interesting as a case-study: several clusters of ceramic sherds have been identified along the edges and within the plateaus on the south-eastern and eastern sides of the crater, probably ascribing to small villages of huts (Guaitoli, 1981). This occupation phase is entangled with the emergence of the two known cemeteries within the GOOCD (Fig. 2): Castiglione, inside the crater rim on the eastern slope, partly overlapping and damaging the Bronze Age settlement, and Osteria dell'Osa, on the western side of the crater along the ancient Praenestina, nearby the Osa Stream. Castiglione is a small cemetery which, chronologically, only overlaps with the earliest phase (9th century B.C.) of the much larger Osteria dell'Osa: there, about 600 burials were excavated dating up to the whole 7th century (Orientalizing Period) and constituting the largest Iron Age burial sample of ancient Latium, while early 6th century votive offerings have been interpreted as markers for the latest period of use of the cemetery (Bietti Sestieri, 1992).

During the course of the Early Iron Age, the inhabitants of the area condensed their settlements in the southern part of the eastern plateau where a proto-urban settlement was established (Pacciarelli, 2010). During the 7th and 6th centuries B.C., the site evolved into an urban settlement with sanctuaries (Zuchtriegel, 2012) and political buildings (Fabbri *et al.*, 2010; Fabbri and Musco, 2016). The fortified city prospered during the Archaic period, but ultimately diminished in importance, power and population from the beginning of the mid-Republican period, 4th/3rd century B.C. (Guaitoli, 2003). Via the Osa Stream and the Aniene River, which flows into the Tiber at ancient Antemnae, Gabii was directly connected to Rome. By the 2nd century B.C., the local tuff rock (Farr *et al.*, 2015) was systematically being mined at Gabii, shipped to the quickly growing city of Rome and used as a building stone (the so-called Lapis Gabinus) on a rather grand scale (Panei and Dell'Orso, 2008).

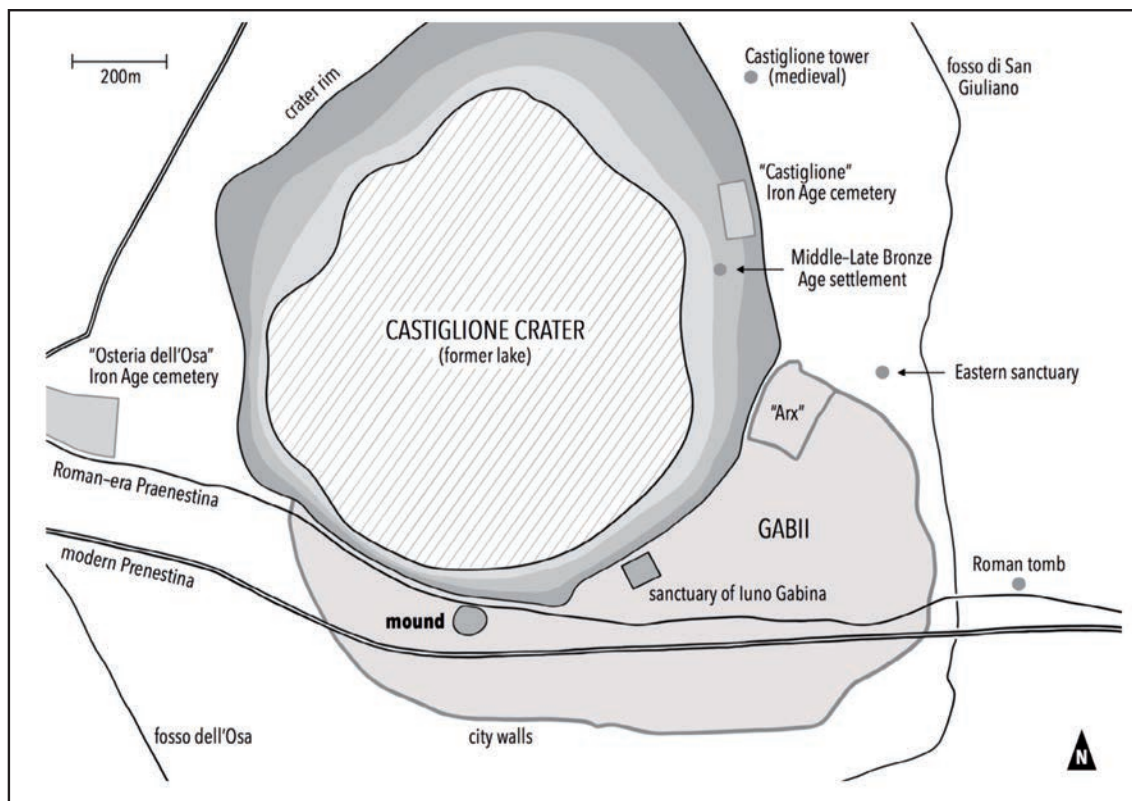


Fig. 2 - Schematic map of the GOOCD with location of the main archaeological evidence including the reconstructed trace of the urban walls perimeter [after Bietti Sestieri (1992) and Helas (2010)].

2.2. Geological setting

The ancient town of Gabii is located on the rim of the Castiglione crater, one eruptive vent of the Colli Albani Volcanic District (CAVD), which is part of the Roman Magmatic Province (Peccerillo, 2005). The CAVD activity took place in three main phases marked by different eruptive mechanisms and magma volumes (e.g. Giordano *et al.*, 2006). The Tuscolano - Artemisio phase produced five geochronologically distinct, large pyroclastic flow sequences in the time span 561-351 ka (Marra *et al.*, 2009; Gaeta *et al.*, 2016), accompanied by minor effusive activity.

The Tuscolano - Artemisio caldera and associated scoria cones developed at the end of this phase of activity, from ca. 365 to 351 ka (Marra *et al.*, 2003). An intermediate, less energetic phase, characterized by Strombolian activity at the central Monte delle Faete edifice and effusive eruptions and subordinate hydromagmatic activity from peripheral vents occurred at 308-250 ka (Marra *et al.*, 2003). Large leucititic lava flows were erupted during this phase, while hydromagmatic surge eruptions occurred at the Castiglione crater [ca. 285 ka: Marra *et al.* (2003)]. Lapis Gabinus (peperino) is the product of these pyroclastic surge eruptions and it is characterised by a relatively high proportion of rock and crystals fragments. A ca. 50-ka long dormancy preceded the start of the late hydromagmatic phase (ca. 200-36 ka), which was dominated by maar and tuff ring forming eruptions. The Albano maar hosted the most recent and voluminous activity of this phase between 69 and 36 ka (Freda *et al.*, 2006; Giaccio *et al.*, 2009).

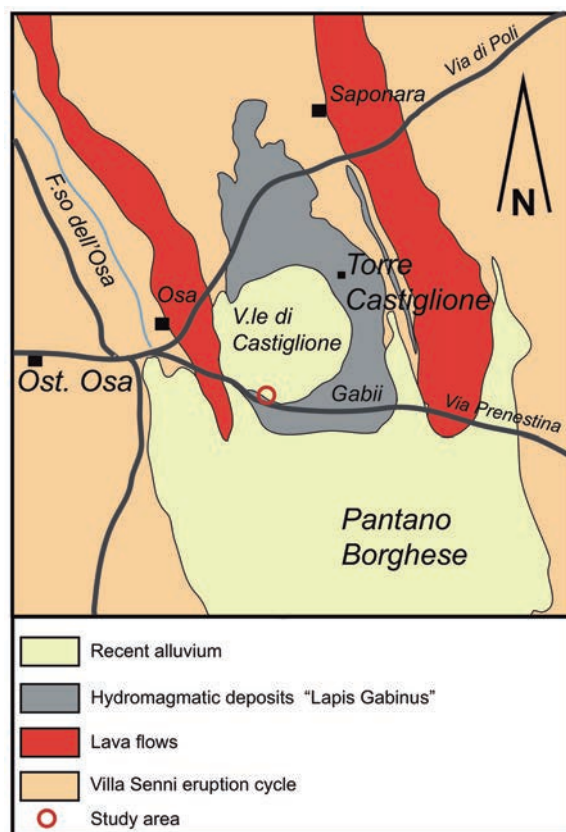


Fig. 3 - Schematic geological map of the area based on sheet 150 "Roma" of the 1:100,000 Carta Geologica d'Italia (available online at: <193.206.192.231/carta_geologica_italia/tavoletta.php?foglio=150>, last consulted on 14.02.2018).

Fig. 3 shows a geological map of the Castiglione area where the main outcropping lithological units are illustrated and described.

3. Methods and results

3.1. Magnetic survey

We carried out a magnetic survey covering the whole *mound* and the surrounding area (Fig. 1). Data acquisition was performed by means of a scalar magnetometer powered by Geometrics, with a sensor placed at about 1.1 m above the ground. Due to survey logistics and constraints related to the presence of diffuse vegetation, magnetic data were acquired in discrete mode over the *mound*, using an integrated GPS receiver for the point measurements georeferencing (UTM projection, WGS84 coordinate system). The digital elevation model of the *mound* area is shown in Fig. 4a. In the surrounding area, magnetic measurements were acquired in continuous mode, using a sampling rate of 1 Hz, along parallel paths about 2 m spaced.

Data processing consisted in removal of spikes and of striping effects between survey lines using the MagMap2000 software tools (Geometrics, 2010). For the *mound* area, we present the contour map of the total magnetic anomaly field (hereinafter TMI; Fig. 4b). TMI data were obtained by removing the main field for the longitude, latitude, and time (as derived from:

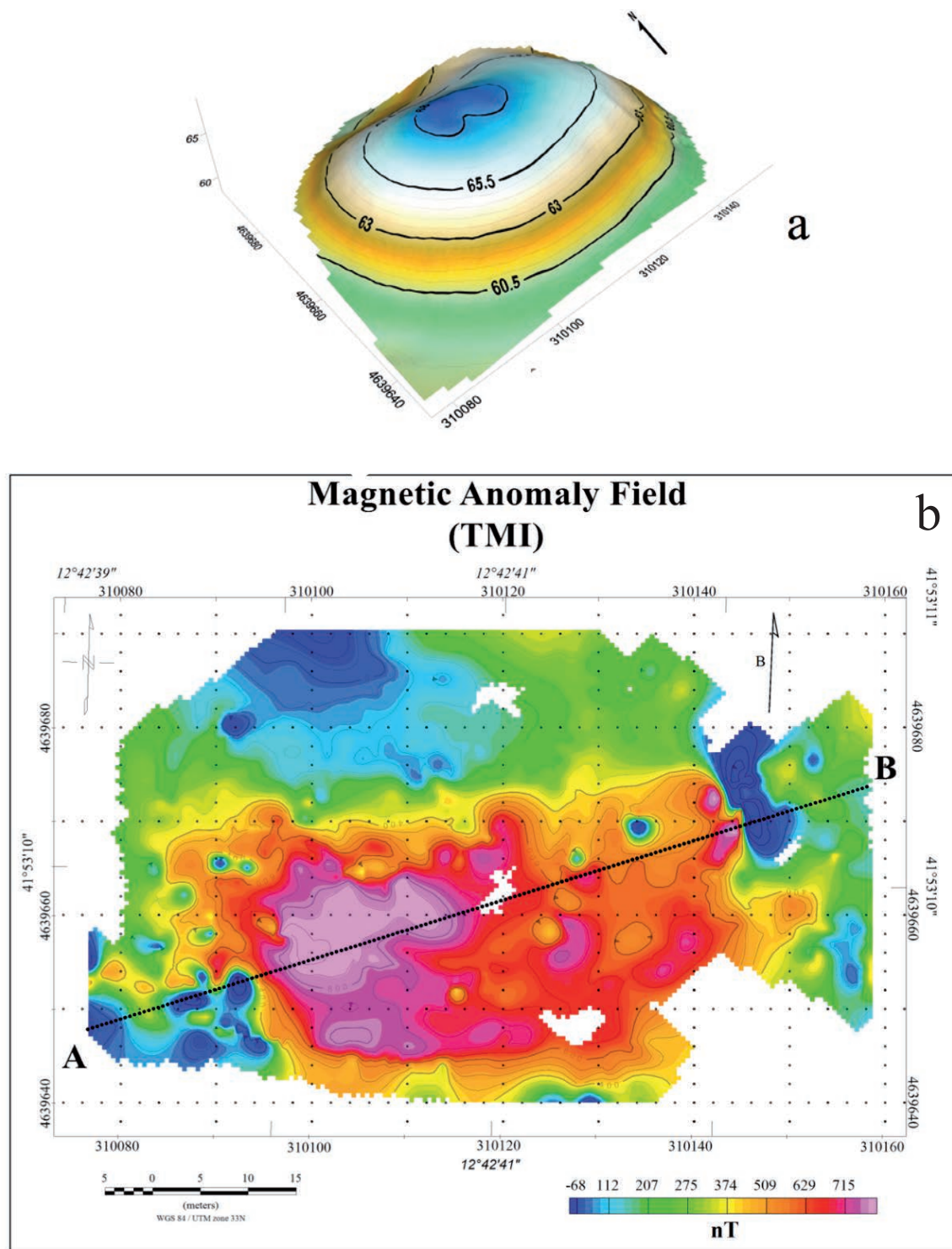


Fig. 4 - a) Digital Elevation Model of the mound; b) Total Magnetic Intensity (TMI) map with the direction of the present day Earth magnetic field (B) and c) Reduced-to-Pole map (RTP-TMI). The RTP transformation has been computed considering an inducing magnetic field inclination and declination of 58 and 2.5° respectively. In panels (b) and (c) contour lines with major intervals at 200 nT are shown. Section A-B in panel (b) indicate the profile track used for the forward model.

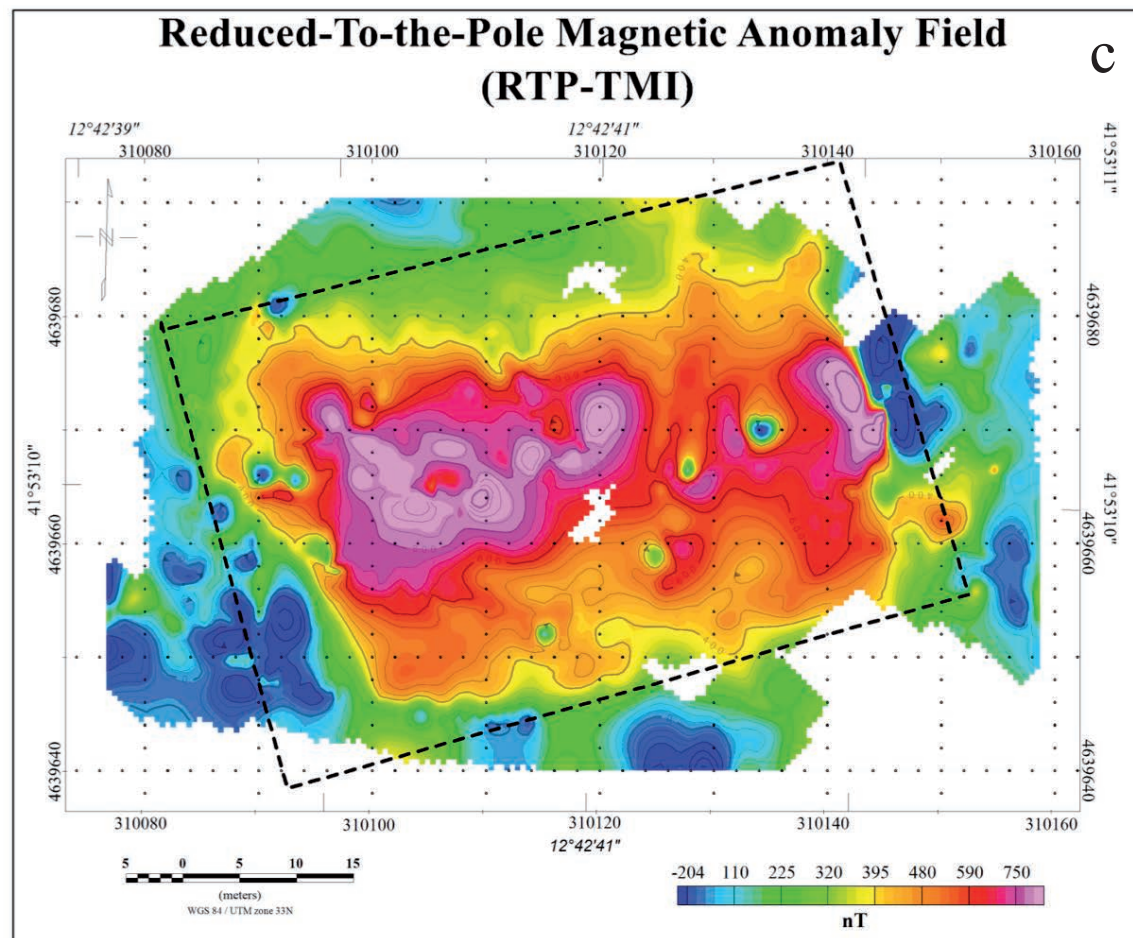


Fig. 4 - continued.

<https://www.ngdc.noaa.gov/geomag-web/#igrfwmm>) and the diurnal variations (using the top sensor as permanent recording station) from the magnetic measurements. Reduced data were also microlevelled in order to remove the lasting small scale errors in the data set (Ferraccioli *et al.*, 1998). TMI map is, then, obtained by interpolating processed magnetic data by means of the Kriging algorithm using a regular cell grid of 6×6 m².

The TMI map shows a clear dipolar magnetic anomaly with intensity ranging from 950 to -740 nT. The TMI field has a strong intensity and is characterized by the superimposition of two components. The main component is represented by the longer wavelength anomaly, almost N-S oriented, according to the present day B field directions. The second component is due to shorter wavelength anomalies, mainly concentrated in the eastern and western sides of the map, forming a complex pattern of coalescing smaller sized magnetic dipoles. It is worth to note that the eastern flank of the *mound* is characterized by the presence of an intense, NE-SW oriented, shorter wavelength dipolar magnetic anomaly approximately orthogonal (70°) to the present day B field direction.

In general, the dipolar nature of magnetic anomalies makes magnetic interpretation difficult, especially when the effects of adjacent sources overlap. In order to facilitate this task, the TMI

grid was Reduced-to-Pole (RTP-TMI in Fig. 4c) using the Oasis Montaj software by Geosoft and considering the actual Earth main field angular values with an inclination of 58° and a declination of 2.8° (Baranov and Naudy, 1964). This analytical transformation centres the magnetic anomalies on their relative sources assuming the absence of remanent magnetizations. As a consequence, the spatial relation between the anomalies (directly polarized) and their sources is improved. This transformation effectively transformed the magnetic effect of the *mound* sources with prevailing induced component N-S aligned, while it left unaltered the fields caused by source with stronger remanence and different orientation from the present day directions. The RTP-TMI map surprisingly changes the shape of the longer wavelength anomaly, forming a rectangular like-shape geometry encompassing the entire *mound* perimeter.

Fig. 5 shows the results of the magnetic survey performed in the area surrounding the *mound*. It is clearly evident the presence of high intense, lined-up and E-W oriented, dipolar magnetic anomalies throughout the survey area and in correspondence of some emerging leucititic lava stones.

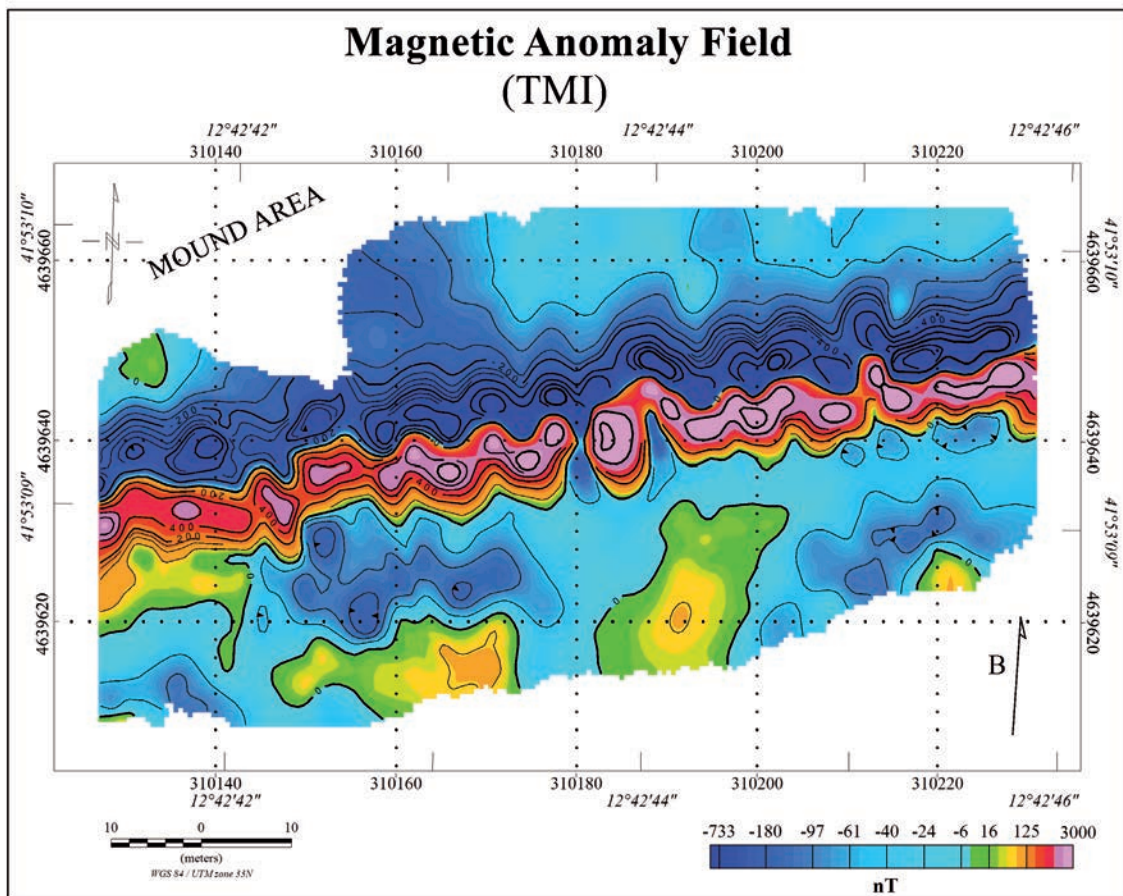


Fig. 5 - Total Magnetic Intensity (TMI) map of the area immediately SE of the *mound*. Contour lines with major intervals at 200 nT are shown.

3.2. Sampling and laboratory measurements

We collected rock (peperino) samples from four notable volcanic units emerging in the study area and its near surrounding in order to characterize their magnetic properties in addition to their mineralogical type and contents. Samples S1 to S4 were collected respectively from four outcrops (see Fig. 1 for their location): outcrop O1 lies about 250 m W-NW of the *mound*; O2 is at the very base of the *mound*, on its eastern flank; O3 lies very close to the Gabii archaeological site, not far from the remains of the temple of Iuno Gabina, about 320 m E-NE of the study area; the last outcrop, O4, is the closest to O2 (no more than 30 m distance in the north direction) and was found on the northern side of the modern car track.

On-field, susceptibility measurements of outcropping rocks were carried out using a portable SM-30 magnetic susceptibility meter by ZH-instruments characterized by an high sensitivity (1×10^{-7} SI units). Several measurements were collected and averaged to get a representative value for each outcrop (S1 = 0.0140 SI, S2 = 0.030 SI, and S3 = 0.0134 SI).

The magnetic mineralogy measurements of the four collected samples were performed at the paleomagnetism laboratory of the Istituto Nazionale di Geofisica e Vulcanologia (INGV), Rome. The hysteresis properties of powders from the four crushed samples have been measured on a Princeton Measurements Corporation 3900 vibrating sample magnetometer (VSM), in fields up to 1 Tesla (T). The coercive force (B_c), the saturation remanent magnetization (M_{rs}), as well as the saturation magnetization (M_s) have been determined after subtracting the high field linear trend; the mass specific values of M_{rs} and M_s have been calculated dividing the measured values for the weight of the samples. The values of the coercivity of remanence (B_{cr}), have been extrapolated from the backfield remagnetization curves after the application of fields up to -1 T, following the forward magnetization in a +1 T field. The variation of the magnetic susceptibility with temperature was measured on the same powders by means of the AGICO MFK1 Kappabridge coupled to a CS-3 furnace. Samples were heated up to 700° C and cooled back to 40° C to estimate the Curie range of temperatures, and to examine any possible mineralogical changes associated with the heating process in air. The magnetic grain-size of the samples has been inferred by means of the “Day Plot” (Dunlop, 2002a, 2002b), according to the saturation remanence to saturation magnetization (M_{rs}/M_s) vs. remanent coercive force to coercive force (B_{cr}/B_c) ratios.

3.3. Magnetic properties results

Hysteresis loops, IRM acquisition curves and backfield applications (Fig. 6) are well defined, due to the relatively high values of the concentration dependent magnetic parameters. The results are consistent with a prevailing low-coercivity component, as evidenced by B_{cr} values, which are in the range 30-35 mT and can be referred to titanomagnetite and/or magnetite, as confirmed by the thermomagnetic data. The susceptibility vs. temperature cooling curves are generally similar or below the heating curve in both samples, indicating limited formation of new ferrimagnetic minerals during the heating process. Ti-poor titanomagnetite results as the main magnetic mineral, with estimated Curie temperatures ranging from 440° to 560° C. The presence of magnetite and/or low-Ti content titanomagnetite is common in these and similar units, as observed in the peperino units from Albano area (Porreca *et al.*, 2008). Titanomagnetite normally occurs both as magmatic free grains and as inclusions in other phenocrysts and glass shards.

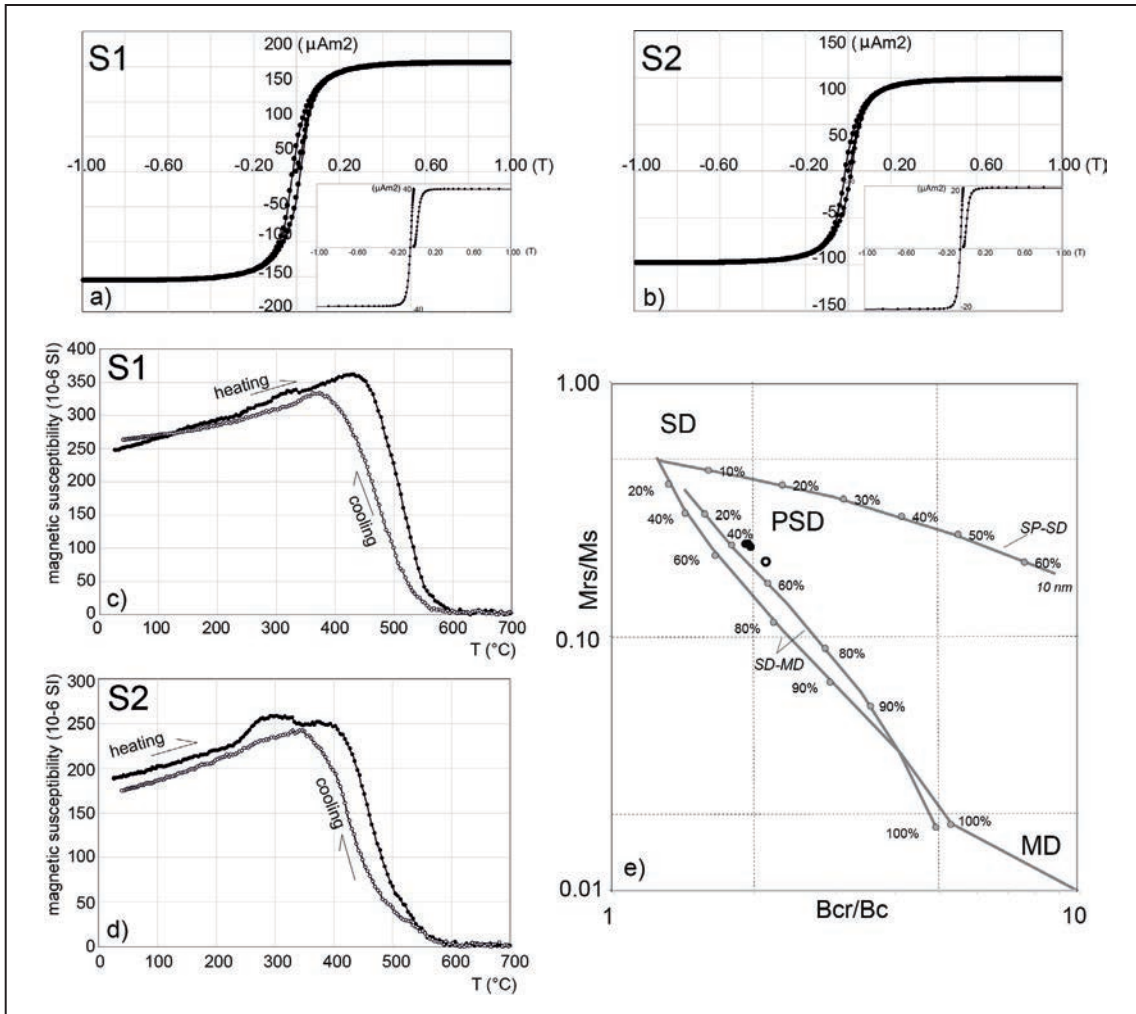


Fig. 6 - Magnetic mineralogy results. Hysteresis loop for samples S1 (a) and S2 (b), corrected for the high field linear trend; in the insets the isothermal remanent magnetization acquisition curve and backfield application. Thermomagnetic curves and backfield application for samples S1 (c) and S2 (d). Magnetic susceptibility data are corrected for the empty furnace. Bi-logarithmic “Day plot” of the hysteresis ratios M_{rs}/M_s vs. B_{cr}/B_c (e). The SD (single domain), PSD (pseudo-single domain) and MD (multidomain) fields and the theoretical mixing trends for SD-MD and SP-SD grains (SP, superparamagnetic) are from Dunlop (2002a, 2002b), and refer to magnetite.

About the magnetic mineral grain-size, all the samples are located in the upper-central region of the “Day plot” (Fig. 6e), between the 40% and the 60% of volume fraction of coarser multidomain (MD) grains in mixture with fine single-domain (SD) particles according to the theoretical trends calculated for mixtures of magnetite grains (Dunlop, 2002a).

4. Magnetic source modelling

In order to evaluate the possible depths, dimension and geometrical characteristics of the TMI sources, we carried out a forward modelling on the TMI field. The 2.75D magnetic modelling was

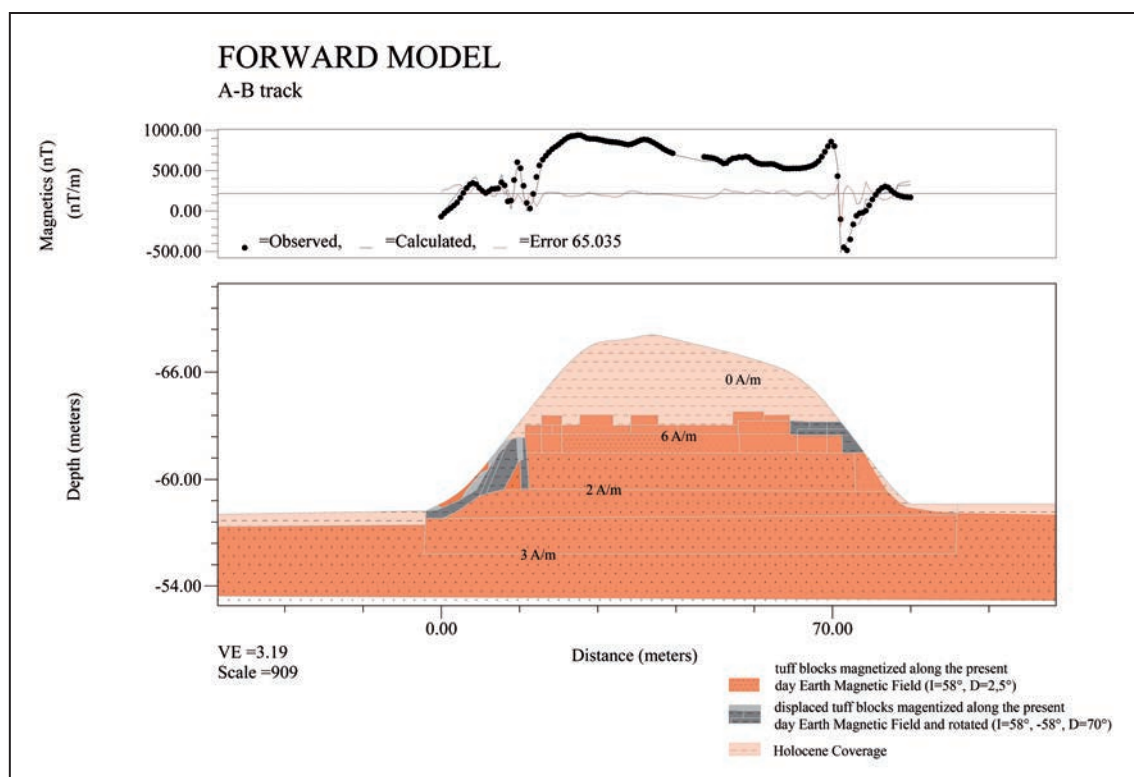


Fig. 7 - Forward magnetic model of the mound along the A-B profile track shown in panel (b) of the Fig. 4. The upper panel reports the values of the observed (point) and computed (black line) magnetic fields and their differences (error - red line) respectively. The lower panel reports the geometrical configuration of the magnetic sources along the x axis (distance from the point A) respect to the depth (altitude above the sea level- minus sign is a computational convention). Source averaged values of the total magnetization ($J_i + J_r$) are also reported for the sequence of layers composing the model.

carried out with the GM-SYS package of Oasis Montaj by Geosoft which uses an implementation of the algorithm obtained by Talwani and Heirtzler (1964) and Rasmussen and Pedersen (1979) and the algorithm proposed by Won and Bevis (1987).

In Fig. 7, we show the modelling results for a profile trace which was purposely chosen in order to cut the maximum of the main anomaly while, at the same time, including the western and the eastern, highest intensity anomalies, respectively.

In order to extract reliable information from the model, we constrained the magnetization of the source bodies with an average susceptibility value that we extrapolated from the measurements in the field.

These values yield to an induced magnetization of about 1.1 A/m for the local intensity of the Earth magnetic field. As for the remanent magnetization (J_r), we assigned the values which are required to fit the computed and the observed magnetic fields with an iterative trial-and-errors process. In this way, we estimated J_r values ranging from 1 A/m to 7 A/m that were attributed to the block sources composing the model.

The magnetic model is characterized by a sequence of layers which tapers going upwards. The total magnetization ($J_i + J_r$), expressing the compressive magnetic properties of the rocks, roughly

increases in the upper levels. In Fig. 7 these magnetic properties are reported as an average value for each layer. At the base of the *mound*, below the recent coverage (with null magnetization) the basal layers have an average magnetization of about 3 A/m, while the first two layers at the bottom of the *mound* have both an average magnetization of 2 A/m. In the last two upper layers the magnetization increases to an average of 6 A/m.

Magnetic modelling reveals that the longer wavelengths are caused by a basal massive plateau magnetized along the present-day Earth magnetic field direction (www.ngdc.noaa.gov) for the latitude of the study area ($I=58^\circ$ and $D=2.5^\circ$). This basal plateau covers the entire *mound* extension along the profile, its upper surface lies 3 m above the base of the *mound* and at about 4 m below its surface.

A sequence of small scale prisms placed on top of the basal plateau and characterized by a susceptibility equal to 0.03 SI, coherent with on-field measurements (corresponding to 1.1 A/m for the induced magnetization J_i) fits the shorter wavelengths of the observed magnetic field. These prisms likely represent small scale stone masses, some of which are characterized by magnetic dipoles with their axis misaligned with the present day induction B field. This is the case, for example, of the outcrop in the eastern flank of the *mound*, whose magnetic dipole axis is rotated about 70° eastwards compared to the N-S direction. Instead, the *mound* western flank shows a sequence of coalescing dipoles with inverted and casually rotated polarities suggesting a chaotic cluster of masses spread on this side of the hill.

5. Discussion and conclusions

The Castiglione *mound* lies within a complex and rich archaeological area. Its proximity with the ancient Praenestina makes it a 'monument' sitting in a position of absolute prominence and importance, overwatching whoever treads the ancient road. Because of these facts, questioning what might be its origin and nature is crucial to ameliorate the general understanding of the archaeological district and its chronological development.

Laboratory measurements have proved to be crucial for the discrimination and characterization of mineralogical contents and the magnetic properties of the volcanic units sampled in the survey area and in its surrounding. The magnetic mineralogy indicates that Ti-poor titanomagnetite is the main magnetic carrier while the magnetic parameters, both concentration dependent and not, are spread in a very limited span of values. On a deeper level, the sample from the *mound* (S2) shows slightly lower values for all the magnetic parameters, with respect to the other three, including the estimated Curie temperature (440° C). This little difference can be ascribed to a moderate increase in the Ti content of the titanomagnetite, as well as to small variations in the concentration of the magnetic minerals for what concerns Ms and Mrs. Such variations are to be considered in the range of possible variability within Lapis Gabinus and similar units, for example the peperino from Albano (Porreca *et al.*, 2008).

Through geo-archaeological recognition, we observed how the *mound* lies in proximity of the Lapis Gabinus outcrop O4: this outcrop, slightly dipping southwards, appears to be at the same altitude of outcrop O2, which is located at the eastern flank of the *mound* (Fig. 8a, see Fig. 1 for their location). During the months we carried out on-field research and surveys, intensive weathering has furtherly exposed O2, revealing significant signs of human intervention in its



Fig. 8 - a) Panoramic view of the outcrops O4 and O2; b) details of outcrop O2.

shaping: in fact, it is articulated in what seem to be adjoining cubic-shaped blocks, about 1 m wide, with regular edges and substantial presence of tool-marks (Fig. 8b). Magnetic data actually showed us how the stone was artificially altered beyond its mere reshaping: since outcrops O2 and O4 belong to the same volcanic unit (Lapis Gabinus, see geological map in Fig. 3), if they both laid in their natural position they would have provided a magnetic anomaly aligned with the B field direction. Contrarily, the TMI map (Fig. 4b) shows a dipolar magnetic anomaly in correspondence of O2 which is not oriented along the present day Earth magnetic field: it results rotated by about 70° clockwise, this means the rock is not lying in its natural position but was rather displaced.

The RTP map (Fig. 4c) depicts a magnetic source effect (longer wavelength) with nearly-rectangular geometry; this geometry also resembles the shape of the source as recovered by the magnetic model (Fig. 7) across its approximately E-W extension (A-B section in Fig. 4b). This data strongly points towards recognising human intervention in the shaping of such core feature lying within the *mound*. Only depthwise extensive archaeological excavation of the *mound* would, and hopefully will, make it clear whether geological substratum, hence Lapis Gabinus, was shaped in place in a somewhat near-quadrangular manner or whether the remarkable magnetic data is given by results of building activity of some kind. It is not to be excluded that different, overlapping phases of human intervention have led to the present morphology.

The magnetic data also showed other traces of human activity in the very near surroundings: in fact, in the field immediately south of the *mound*, magnetic results showed a series of intense dipolar magnetic anomalies (up to approximately 3000 nT), N-S oriented, arranged to form a linear, E-W oriented pattern. These anomalies are related to the presence of ferromagnetic masses

which we attribute to leucititic lava stones, some of which have emerged and were visible on the ground. It is possible that both the magnetic anomaly and the emerging stones are traces of what remains of an ancient paved road.

Despite our results are encouraging, we claim that modelled and observed magnetic data alone did not really allow us to gather conclusive interpretation of the *mound* and, the magnetic survey itself is not adequate to accurately characterize and discriminate all possible subsurface features within the *mound*, both in the very shallow and at depth. Therefore, we claim that further geophysical surveys would be crucial to ascertain the shallow layers of the *mound* and to accurately characterize the subsoil of the entire area. To this end, in the near future the geophysical survey will be extended to microgravity and 3D electrical resistivity tomography (ERT) measurements. The latter could then be used to build up a 3D resistivity model of the *mound* up to a depth of about 20 m. The microgravity data, on the other hand, will be useful to accurately locate possible voids, cavities (also partially filled) and any excesses or losses of masses based on measured density contrast within the *mound*. Our idea is to perform a microgravity survey, with a regular grid (5 m spaced) of acquisition, with the aim to detect spherical-shaped cavities, approximately 2-3 m wide or even greater (i.e. Di Filippo *et al.*, 2005; Braitenberg *et al.*, 2016). In addition, taking into account that the main geological unit of the survey area (Lapis Gabinus) has a density of 1550 kg/m³ (Ventriglia, 2002) and assuming that the top of possible buried structures lies in the very near surface, it would also be possible to detect whether the cavity is void or filled by sediments with a minimum gravity variation in signal from 20 to 50 μ Gal.

Acknowledgments. The authors kindly thank the reviewer Carla Braitenberg for the precious revision which significantly improved the manuscript. We thank Micaela Angle (Soprintendenza Archeologica del Lazio e dell'Etruria Meridionale) for allowing and supporting this research. Special thanks also go to the friends in Gruppo Archeologico Latino (G.A.L.) "Latium Vetus" and particularly to its director, Enrico Devoti, for the precious assistance during our fieldwork. Thanks to the owners of the land where the *mound* lies for allowing the scientific surveys and to Marco Marchetti (Istituto Nazionale di Geofisica e Vulcanologia) for encouraging this study.

REFERENCES

- Aglietti S.; 2002: *La via dei Cavoni nel Lazio medievale*. In: Patitucci Uggeri S. (ed), *La viabilità medievale in Italia: contributo alla carta archeologica medievale* (Quaderni di archeologia medievale IV), All'Insegna del Giglio, Firenze, Italy, pp. 181-196.
- Angle M. and Mancini D.; 2010: *Pantano Borghese: un insediamento protostorico ai margini della palude*. In: *Archeologia e infrastrutture, Il tracciato fondamentale della Linea C della metropolitana di Roma: prime indagini archeologiche*, Bollettino d'Arte del Ministero per i Beni e le Attività Culturali, Olschki, Firenze, Italy, pp. 293-314.
- Baranov V. and Naudy H.; 1964: *Numerical calculation of the formula of reduction to the magnetic pole*. *Geophys.*, **29**, 67-79.
- Becker J.A., Mogetta M. and Terrenato N.; 2009: *A new plan for an Ancient Italian City: Gabii revealed*. *Am. J. Archaeol.*, **113**, 629-642, doi:10.3764/aja.113.4.629.
- Bietti Sestieri A.M.; 1992: *The iron age community of Osteria dell'Osa: a study of socio-political development in central Tyrrhenian Italy*. Cambridge University Press, Cambridge, UK, 284 pp.
- Braitenberg C., Sampietro D., Pivetta T., Zuliani D., Barbagallo A., Fabris P., Rossi L., Fabbri J. and Mansi A.H.; 2016: *Gravity for detecting caves: airborne and terrestrial simulations based on a comprehensive karstic cave benchmark*. *Pure Appl. Geophys.*, **173**, 1243-1264, doi:10.1007/s00024-015-1182-y.
- Cozza A. and Pasqui A.; 1885: *Gabii (Agro Romano), Notizie degli scavi*. NSA 1885, pp. 424-428.

- Di Filippo M., Di Nezza M., Marchetti M., Urbini S., Toro A. and Toro B.; 2005: *Geophysical research on Via Appia: the so-called "Monte di Terra" funeral monument*. In: Proc. 6th Int. Conf. Archaeolog. Prospect., Nat. Res. Council, Roma, Italy, pp. 292-294.
- Dunlop D.; 2002a: *Theory and application of the Day plot (Mrs/Ms versus Hcr/Hc) 1. Theoretical curves and tests using titanomagnetite data*. J. Geophys. Res., **107**, 2056, doi:10.1029/2001JB000486
- Dunlop D.; 2002b: *Theory and application of the Day Plot (Mrs/Ms versus Hcr/Hc) 2. Application to data for rocks, sediments, and soils*. J. Geophys. Res., **107**, 2057, doi:10.1029/2001JB000487.
- Fabbri M. and Musco S.; 2016: *Nuove ricerche sulle fortificazioni di Gabii. I tratti nord-orientale e settentrionale*. In: Atti Giornate di Studio Accademia Belgica, Fontaine P. and Helas S. (eds), *Le fortificazioni arcaiche del Latium vetus e dell'Etruria meridionale (IX - VI sec. a. C.). Stratigrafia, cronologia e urbanizzazione*, Istituto Storico Belga, Roma, Italy, pp. 71-90.
- Fabbri M., Musco S. and Osanna M.; 2010: *Sur les traces des Tarquins à Gabies. Une découverte exceptionnelle*. Les Dossiers d'Archéologie, **339**, 62-65.
- Farr J., Marra F. and Terrenato N.; 2015: *Geochemical identification criteria for "peperino" stones employed in ancient Roman buildings: a Lapis Gabinus case study*. J. Archaeolog. Sci.: Reports, **3**, 41-51, doi:10.1016/j.jasrep.2015.05.014.
- Ferraccioli F., Gambetta M. and Bozzo E.; 1998: *Microleveling procedures applied to regional aeromagnetic data: an example from Transantarctic Mountains (Antarctica)*. Geophys. Prospect., **46**, 177-196.
- Freda C., Gaeta M., Karner D.B., Marra F., Renne P.R., Taddeucci J., Scarlato P., Christensen J.N. and Dallai L.; 2006: *Eruptive history and petrologic evolution of the Albano multiple maar (Alban Hills, central Italy)*. Bull. Volcanol., **68**, 567-591, doi:10.1007/s00445-005-0033-6.
- Gaeta M., Freda C., Marra F., Arienzo I., Gozzi F., Jicha B. and Di Rocco T.; 2016: *Paleozoic metasomatism at the origin of Mediterranean ultrapotassic magmas: constraints from time-dependent geochemistry of Colli Albani volcanic products (central Italy)*. Lithos, **244**, 151-164, doi:10.1016/j.lithos.2015.11.034.
- Geometrics; 2010: *MagMap2000™ & MagPick™. Essential data processing procedures and operational review*. Geometrics Inc., San Jose, CA, USA, <geometrics.com>.
- Giaccio B., Marra F., Hajdas I., Karner D.B., Renne P.R. and Sposato A.; 2009: *40Ar/39Ar and 14C geochronology of the Albano maar deposits: implications for defining the age and eruptive style of the most recent explosive activity at the Alban Hills Volcanic District, Italy*. J. Volcanol. Geoth. Res., **185**, 203-213, doi:10.1016/j.jvolgeores.2009.05.011.
- Giordano G., De Benedetti A.A., Diana A., Diano G., Gaudio F., Marasco F., Miceli M., Mollo S., Cas R.A.F. and Funicello R.; 2006: *The Colli Albani mafic caldera (Roma, Italy): stratigraphy, structure and petrology*. J. Volcanol. Geoth. Res., **155**, 49-80.
- Guaitoli M.; 1981: *Osservazioni sulle fasi di sviluppo dell'abitato*. Quaderni dell'Istituto di topografia antica, **10**, 23-57.
- Guaitoli M.; 2003: *Gabii (Roma)*. In: Guaitoli M. (ed), *Lo sguardo di Icaro: le collezioni dell'aerofototeca nazionale per la conoscenza del territorio*, Campisano, Roma, Italy, pp. 273-277.
- Helas S.; 2010: *Prospezioni geofisiche a Gabii: interpretazioni e prospettive per uno studio delle mura*. In: Atti Sesto Incontro di Studi sul Lazio e la Sabina, G. Ghini (ed), Lazio e Sabina 6, pp. 249-258.
- Ioane D., Anghel S. and Dudu A.; 2009: *Magnetic prospection of a Tumulus in the Ancient Histria Necropolis*. GEO-ECO-MARINA, Sedimentary processes and deposits within River-Sea Systems, **15**, 161-165.
- Marra F., Freda C., Scarlato P., Taddeucci J., Karner D.B., Renne P.R., Gaeta M., Palladino D.M., Trigila R. and Cavarretta G.; 2003: *40Ar/39Ar Geochronology of the recent phase of activity of the Alban Hills Volcanic District (Roma, Italy): implications for seismic and volcanic hazards*. Bull. Volcanol., **65**, 227-247, doi:10.1007/s00445-002-0255-9.
- Marra F., Karner D.B., Freda C., Gaeta M. and Renne P.R.; 2009: *Large mafic eruptions at the Alban Hills Volcanic District (central Italy): chronostratigraphy, petrography and eruptive behavior*. J. Volcanol. Geoth. Res., **179**, 217-232, doi:10.1016/j.jvolgeores.2008.11.009.
- Pacciarelli M.; 2010: *Dal villaggio alla città: la svolta protourbana del 1000 a. C. nell'Italia tirrenica*. Grandi contesti e problemi della protostoria italiana, All'Insegna del Giglio, Firenze, Italy, 310 pp.
- Panei L. and Dell'Orso M.; 2008: *I tufi delle Mura Serviane: origini e caratterizzazione chimico-mineralogica*. In: Barbera M. and Magnani Cianetti M. (eds), *Archeologia a Roma Termini: le mura serviane e l'area della stazione: scoperte, distruzioni e restauri*, Electa, Roma, Italy, pp. 96-107.
- Peccerillo A.; 2005: *Plio-Quaternary volcanism in Italy: petrology, geochemistry, geodynamics*. Springer-Verlag, Berlin, Germany, 365 pp., doi:10.1007/3-540-29092-3.

- Pinza G.; 1903: *Gabii ed i suoi monumenti*. *Bullettino della Commissione Archeologica Comunale di Roma*, **31**, 321-364.
- Porreca M., Mattei M., Macniocai C., Giordano G., McClelland E. and Funicello R.; 2008: *Paleomagnetic evidence for low-temperature emplacement of the phreatomagmatic peperino Albano ignimbrite (Colli Albani Volcano, central Italy)*. *Bull. Volcanol.*, **70**, 877-893, doi:10.1007/s00445-007-0176-8.
- Rasmussen R. and Pedersen L.B.; 1979: *End corrections in potential field modelling*. *Geophys. Prospect.*, **27**, 749-760.
- Talwani M. and Heirtzler J.R.; 1964: *Computation of magnetic anomalies caused by two-dimensional bodies of arbitrary shape*. In: Parks G.A. (ed), *Computers in the mineral industries*, Stanford Univ. Press, Stanford, CA, USA, pp. 464-480.
- Ventriglia U.; 2002: *Caratteristiche geotecniche dei terreni del Comune di Roma*. In: *Geologia del territorio del Comune di Roma*, Casa Editrice Cerbone, Afragola (Na), Italy, pp. 39-106.
- Won I.J. and Bevis M.; 1987: *Computing the gravitational and magnetic anomalies due to a polygon: algorithms and Fortran subroutines*. *Geophys.*, **52**, 232-238.
- Zuchtriegel G.; 2012: *Gabi I. Das Santuario Orientale im Zeitalter der Urbanisierung*. Osanna ed., Venosa (Pz), Italy, 404 pp.

Corresponding author: Vincenzo Sapia
Istituto Nazionale di Geofisica e Vulcanologia
Via di Vigna Murata 605, 00143 Roma, Italy
Phone: +39 06 51860723; e-mail: vincenzo.sapia@ingv.it